

See discussions, stats, and author profiles for this publication at: <https://www.researchgate.net/publication/260716433>

# Coordination versus Solvation in $\text{Al}^+$ (benzene)(n) Complexes Studied with Infrared Spectroscopy

ARTICLE in THE JOURNAL OF PHYSICAL CHEMISTRY A · MARCH 2014

Impact Factor: 2.69 · DOI: 10.1021/jp500778w · Source: PubMed

---

CITATION

1

---

READS

23

4 AUTHORS, INCLUDING:



Jonathan D Mosley

United States Environmental Protection Agency

12 PUBLICATIONS 39 CITATIONS

SEE PROFILE

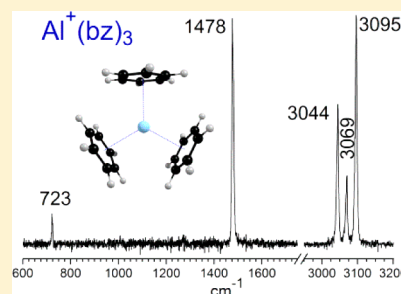
# Coordination versus Solvation in $\text{Al}^+(\text{benzene})_n$ Complexes Studied with Infrared Spectroscopy

Kimberly N. Reishus, Antonio D. Brathwaite, Jonathan D. Mosley, and Michael A. Duncan\*

Department of Chemistry, University of Georgia, Athens, Georgia 30602, United States

**S** Supporting Information

**ABSTRACT:** Singly charged aluminum–benzene cation complexes are produced by laser vaporization in a pulsed supersonic expansion. The  $\text{Al}^+(\text{benzene})_n$  ( $n = 1\text{--}4$ ) ions are mass selected and investigated with infrared laser photodissociation spectroscopy. Density functional theory (DFT) is employed to investigate the structures, energetics and vibrational spectra of these complexes. Spectra in the C–H stretching region exhibit sharp multiplet bands similar to the pattern known for the Fermi triad of the isolated benzene molecule. In the fingerprint region, strong bands are seen corresponding to the  $\nu_{19}$  C–C ring motion and the  $\nu_{11}$  out-of-plane hydrogen bend. The hydrogen bend is strongly blue-shifted compared to this vibration in benzene, whereas the  $\nu_{19}$  carbon ring distortion is only slightly shifted to the red. Computed structures and energetics, together with experimental fragmentation and vibrational patterns, indicate a primary coordination of three benzene molecules around the central  $\text{Al}^+$  cation. The  $n = 4$  complex contains one second-sphere solvent molecule.



## INTRODUCTION

Metal–benzene complexes provide prototypical examples of organometallic bonding and cation– $\pi$  interactions.<sup>1–8</sup> The spectroscopy and chemistry of these systems have been studied for many years in the condensed phase, due to their relevance for homogeneous catalysis.<sup>1–3</sup> A renewed interest in these complexes has been stimulated by the importance of cation– $\pi$  interactions in supramolecular chemistry and biological systems.<sup>4–8</sup> The fundamental details of bonding patterns, charge transfer, and progressive solvation have been studied in gas phase systems, which can be compared more directly with computational results.<sup>9–18</sup> In the present report, we investigate gas phase aluminum cation–benzene complexes using infrared photodissociation spectroscopy and computational chemistry.

The most common structure for metal benzene complexes is the dibenzene sandwich.<sup>1,2</sup>  $\text{Cr}(\text{benzene})_2$  is the classic example of this structure, and its stability is attributed at least in part to its 18-electron configuration. Ionized analogs that achieve this same closed-shell electronic structure have also been investigated in traditional condensed phase chemistry.<sup>2</sup> Although symmetric sandwich structures are most familiar, when the metal center is electron-rich or electron-poor, deviations from this common motif may occur. Complexes with different numbers of ligands may form, as well as those in which the metal binds in sites with less than the usual 6-fold coordination.<sup>18</sup> These issues have been investigated for transition metal systems, but there is less information for main group metal complexes. In the present study, we explore benzene complexes with the aluminum cation. Unlike transition metal systems, the  $3s^2$  valence configuration of  $\text{Al}^+$  is expected to lead to bonding interactions with benzene that are primarily

electrostatic in nature. It is less clear what the coordination and structures will be for these systems.

Gas phase metal ion–benzene complexes have been studied extensively to probe the fundamental bonding interactions in these systems. Formation processes and reactions have been investigated under different conditions in mass spectrometry.<sup>13,18–22</sup> Collision-induced dissociation,<sup>23–27</sup> radiative association,<sup>28</sup> and photodissociation<sup>29–37</sup> measurements have explored cation–benzene bond energies. Spectroscopy studies have included tunable laser electronic photodissociation<sup>32–34,38,39</sup> and photoelectron spectroscopy.<sup>40–45</sup> Perhaps the most informative data about structures and bonding come from infrared photodissociation studies of mass-selected ions.<sup>46–52</sup> Free electron lasers (FELs) have generally been employed for resonance-enhanced multiphoton dissociation (REMPD) studies in the fingerprint region,<sup>47–49</sup> whereas IR optical parametric oscillator (OPO) laser systems have investigated the C–H stretching region,<sup>46,50–52</sup> usually using the method of tagging with rare gas atoms. Computational work has complemented many of these spectroscopic studies.<sup>53–67</sup> Unfortunately, the infrared spectrum of isolated benzene in the C–H stretching region is complicated by the occurrence of a Fermi triad in the vibrational structure.<sup>68</sup> This feature and its response to metal cation binding are not handled with standard harmonic computational methods, limiting the insight that can be gained in this region. Likewise, REMPD vibrational bands in the fingerprint region are often broadened

**Special Issue:** Kenneth D. Jordan Festschrift**Received:** January 22, 2014**Revised:** March 11, 2014**Published:** March 12, 2014

by multiphoton effects, shifting their positions and relative intensities. Benzene vibrations should shift in systematic ways depending on the nature of the bonding and the metal–ligand charge transfer.<sup>57</sup> However, improved spectroscopy on these systems in the fingerprint region is needed to see these effects. In the present study, we investigate the infrared spectroscopy of  $\text{Al}^+(\text{benzene})_n$  complexes ( $n = 1-4$ ). The binding of aluminum cation to small molecules including benzene has been the subject of several previous studies.<sup>28,69–75</sup> The IR spectroscopy of the monoligand  $\text{Al}^+$ –benzene ion has been reported using REMPD with the FELIX free electron laser.<sup>48</sup> Here, we apply photodissociation and the method of rare gas atom tagging in the C–H stretching region, extend these studies into the fingerprint region and to multiligand complexes. Spectral patterns, complemented by computational studies, reveal the unusual coordination in this system.

## EXPERIMENTAL SECTION

Aluminum–benzene ion–molecule complexes, and those with attached argon atoms, are produced by laser vaporization in a pulsed nozzle molecular beam source using the “cutaway” source configuration.<sup>76</sup> Benzene vapor above the liquid at room temperature is entrained in mixtures of helium, neon, and argon to produce an expansion gas mixture used at a nozzle backing pressure of about 10 atm. Ions are sampled into a differentially pumped time-of-flight mass spectrometer, where they are mass analyzed and selected for spectroscopy. Ions are mass selected with pulsed deflection plates and then irradiated at the turning point in a reflectron instrument with a tunable infrared laser system. The instrument configuration for these experiments has been described in detail previously.<sup>77</sup> Mass spectra are recorded with a digital oscilloscope connected to a PC with an IEEE-488 interface. Different configurations of the optical parametric oscillator (OPO) laser system cover the IR regions 2000–4500 and 600–2300  $\text{cm}^{-1}$ .<sup>78,79</sup> The laser line width is about 1  $\text{cm}^{-1}$ ; wavelengths are calibrated with photoacoustic measurements of the spectrum of methane. Spectra are collected by recording the yield of a specific fragment ion versus the laser energy. In the case of  $\text{Al}^+(\text{benzene})_{1-3}$  complexes, which do not fragment efficiently with IR excitation, we use the method of argon tagging.<sup>80–85</sup> The corresponding  $\text{Al}^+(\text{benzene})_{1-3}\text{Ar}$  complex is produced and mass selected, and then the fragment detected following infrared excitation is that corresponding to the loss of the argon. The  $\text{Al}^+(\text{benzene})_4$  complex spectrum is detected in the mass channel corresponding to the loss of benzene.

Computational studies employed density functional theory (DFT). To determine structures and vibrational frequencies, the B3LYP functional was employed as implemented in Gaussian 03.<sup>86</sup> This method has been documented in previous work to provide the most reliable predictions for infrared spectra. To account for dispersion forces influencing molecular geometries and to determine more accurate binding energies, the B97-D functional was employed as implemented in GAMESS.<sup>87,88</sup> The 6-311+G(d,p) basis set was used for both sets of calculations. The energies are not ZPVE or BSSE corrected. For comparison to the experimental infrared spectra, harmonic frequencies were scaled on a mode-by-mode basis using the computed versus experimental frequencies for benzene.<sup>68</sup> Bands in simulated spectra were given a 10  $\text{cm}^{-1}$  fwhm Lorentzian line shape.

## RESULTS AND DISCUSSION

The mass spectrum of complexes produced in this experiment (see Supporting Information) contains primarily ions of the form  $\text{Al}^+(\text{benzene})_n$  and  $\text{Al}^+(\text{benzene})_n\text{Ar}$ . Infrared excitation in the C–H stretching region does not cause photodissociation of the  $\text{Al}^+(\text{benzene})_{1,2}$  complexes, consistent with their relatively high dissociation energies (see below). However, larger complexes beginning with the  $n = 3$  species photodissociate by eliminating intact benzene molecules. The efficiency of this process is quite low for the  $n = 3$  complex, but greater for the larger systems. Figure 1 shows the photodissociation mass

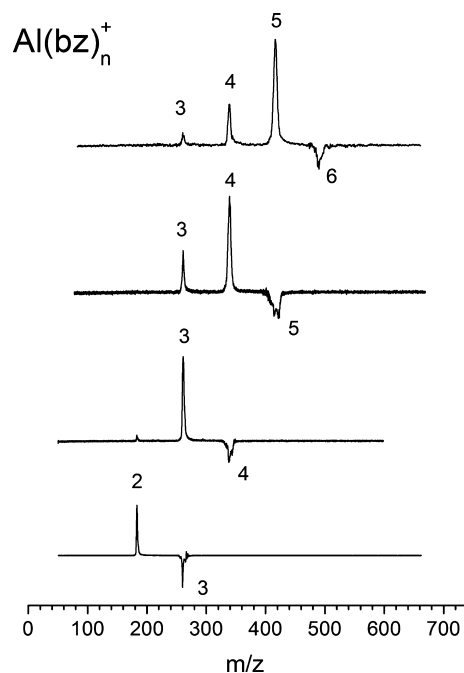


**Figure 1.** Photodissociation mass spectra of  $\text{Al}^+(\text{C}_6\text{H}_6)_n$  complexes, showing the tendency for each cluster to eliminate benzene molecules upon IR excitation.

spectra for these ions, when the laser is tuned to the most intense band of the C–H stretch Fermi triad. The negative peak indicates the depletion of the parent ion and the positive peaks indicate the resulting photofragments. As shown,  $\text{Al}^+(\text{benzene})_3$  loses one benzene to produce  $\text{Al}^+(\text{benzene})_2$ . Likewise,  $\text{Al}^+(\text{benzene})_4$  also loses primarily one benzene, producing an intense signal for  $\text{Al}^+(\text{benzene})_3$  as the fragmentation product.  $\text{Al}^+(\text{benzene})_{5,6}$  each lose a series of benzene molecules terminating at the  $\text{Al}^+(\text{benzene})_3$  ion. This kind of behavior, in which one particular ion survives preferentially in the dissociation processes from different starting ions, has been seen in the past for many metal ion–ligand complexes. Clearly, the details of ligand elimination depend on the ligand binding energy, the photon energy employed, and the number of photons absorbed. However, the behavior here suggests that the coordination around the aluminum cation is complete with three benzene molecules.

To investigate the energetics of these fragmentation processes and the corresponding  $\text{Al}^+(\text{benzene})_n$  structures, we have employed DFT computations. We first used the standard B3LYP functional, which has been shown to be reliable for the determinations of structures and the prediction of vibrational spectra for many transition metal cation–ligand complexes.<sup>89,90</sup>

Then, recognizing that these aluminum cation–benzene complexes may have a significant electrostatic/dispersion component in their bonding, we employed the B97-D functional, which may produce more reliable bond energies for electrostatic systems. The complete results of these calculations are provided in the Supporting Information for this paper. Both functionals produce the same qualitative structures for each of the  $\text{Al}^+(\text{benzene})_n$  ( $n = 1-4$ ) complexes; the B3LYP structures are shown in Figure 2. However, the

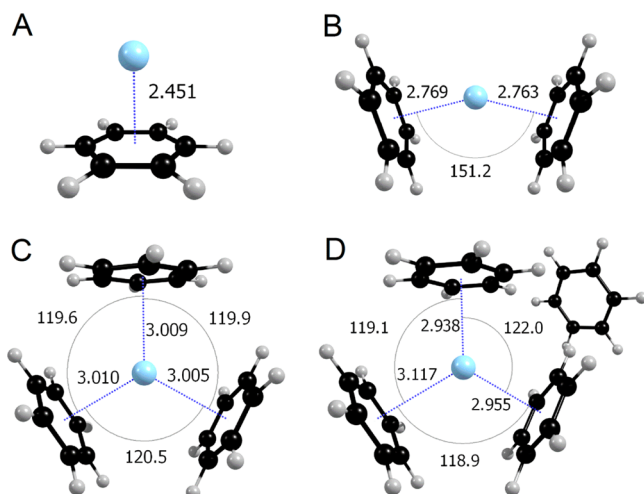


**Figure 2.** Structures predicted for the  $\text{Al}^+(\text{C}_6\text{H}_6)_{1-4}$  complexes at the DFT/B3LYP/6-311+G(d,p) level.

B3LYP versus B97-D structures vary significantly in metal–benzene bond distances (Supporting Information) and in bond energies (Table 1). The monobenzene complex has the

**Table 1. Binding Energies (BE) of the Benzene Ligand (kcal/mol) for  $\text{Al}^+(\text{benzene})_n$  Complexes, Calculated at the DFT/B3LYP and DFT/B97-D Levels Using the 6-311+G(d,p) Basis Set<sup>a</sup>**

| complex                         | B3LYP | B97-D | previous theory   | exp               |
|---------------------------------|-------|-------|-------------------|-------------------|
| $\text{Al}^+(\text{benzene})$   | 30.0  | 35.0  | 35.6 <sup>b</sup> | 35.2 <sup>c</sup> |
| $\text{Al}^+(\text{benzene})_2$ | 11.6  | 20.7  |                   |                   |
| $\text{Al}^+(\text{benzene})_3$ | 4.5   | 14.6  |                   |                   |
| $\text{Al}^+(\text{benzene})_4$ | 2.8   | 10.9  |                   |                   |

<sup>a</sup>The energies are not ZPVE or BSSE corrected. <sup>b</sup>Reference 54.

<sup>c</sup>Reference 28.

aluminum cation binding in the expected 6-fold symmetric site above the benzene ring center. The dibenzene complex has aluminum in a similar site relative to each ring, but the two benzene rings are tilted away from each other and the sandwich structure is distorted from  $D_{6h}$  symmetry. The  $\text{Al}^+(\text{benzene})_3$  complex has three benzene rings all coordinated to the aluminum cation. At each contact point, the metal cation binds in a 6-fold site to benzene, but again the metal is bent out of the plane defined by the centers of the three ligands. To our knowledge, such 3-fold coordination of a metal cation with benzene has been seen previously only in computational work on alkali metal systems.<sup>60–62</sup> In that work, the coordination number varied with the alkali metal ion size, and similar effects may be expected when other main group cation–benzene complexes are studied. The  $\text{Al}^+(\text{benzene})_4$  ion has the same structure as  $\text{Al}^+(\text{benzene})_3$  but with one second-sphere benzene

acting essentially as a solvent molecule. The external benzene is bound primarily by bifurcated  $\pi$ -hydrogen bonds involving C–H groups of two of the inner-sphere molecules directed into the  $\pi$  system of the outer one. This configuration is reminiscent of those seen for the neutral<sup>91</sup> or protonated<sup>92</sup> benzene dimers or for the external benzenes in  $\text{Ni}^+(\text{benzene})_n$  complexes.<sup>65</sup>

The binding energies determined with the two functionals (not corrected for ZPVE or BSSE) are presented in Table 1. The values obtained with the B97-D functional are all significantly higher than those determined with B3LYP, consistent with a significant dispersion component in the bonding. The B3LYP data also exhibit a much steeper falloff in binding energies for the larger complexes. As shown in the table, the B97-D bond energy for the  $\text{Al}^+(\text{benzene})$  complex (35.0 kcal/mol) agrees well with previous computational results<sup>54</sup> and with the experimental value.<sup>28</sup> There are no previous results for the larger complexes. We have done all these calculations at the B3LYP level for complexes with and without argon. As shown in the Supporting Information, argon has virtually no effect on the structures or predicted vibrational frequencies. The predicted spectra shown in the figures throughout the paper are those for complexes without argon.

The bent-sandwich structure for  $\text{Al}^+(\text{benzene})_2$  and the nonplanar configuration of  $\text{Al}^+(\text{benzene})_3$  are perhaps a little surprising, but in fact not unexpected on the basis of previous studies of aluminum ion–molecule complexes. As first described by Bauschlicher,<sup>70</sup> the occupied 3s orbital for  $\text{Mg}^+$ ,  $\text{Al}^+$ , and  $\text{Si}^+$  is highly polarizable, and electron repulsion causes a lobe of electron density to form in the space opposite ligands that bind to these ions. Because of this polarized orbital, second ligands do not bind exactly opposite the first but instead bind in bent positions, and third ligands also avoid the electron density to produce nonplanar complexes. These bent structures have been documented in experiments on the carbonyl and  $\text{CO}_2$  complexes of  $\text{Mg}^+$ ,  $\text{Al}^+$ , and  $\text{Si}^+$ .<sup>93–96</sup> The same effect is seen for the  $\text{Al}^+$  and  $\text{Zn}^+$  cations in complexes with water, which are bent in the same way.<sup>70,74,90</sup>

The wavelength dependence of photodissociation processes such as these can provide their vibrational spectroscopy, and test these predictions of cluster structures. However, as noted above, the small  $\text{Al}^+(\text{benzene})_n$  complexes do not photodissociate, suggesting that their bond energies are greater than the energy of the IR photons used to excite the vibrations. Multiphoton processes are possible in principle, but they are not usually efficient with the pulse energies (<10 mJ/pulse, unfocused) available from our OPO system. We therefore employ the method of rare gas atom tagging<sup>50,80–85</sup> to obtain the spectroscopy of the smaller  $\text{Al}^+(\text{benzene})_n$  complexes. In this method, we produce the  $\text{Al}^+(\text{benzene})_n\text{Ar}$  complexes, and vibrational excitation leads to elimination of argon. Figure 3 shows the spectrum measured in this way for  $\text{Al}^+(\text{benzene})$ , compared to that measured previously for this same ion by our group using multiphoton dissociation with the FELIX free electron laser (FEL).<sup>48</sup> For comparison to these experimental spectra, we present the infrared absorption spectrum predicted with DFT/B3LYP, with vibrations scaled on a mode-by-mode basis, as described above. The dashed red lines correspond to the positions of corresponding vibrational bands in the benzene molecule. As shown in the Supporting Information (Figures S5–S8), spectra predicted with the B97-D functional do not agree with those from B3LYP, nor as well with the experiment, even though mode-specific scaling is employed for each. However, there is reasonably good agreement between the



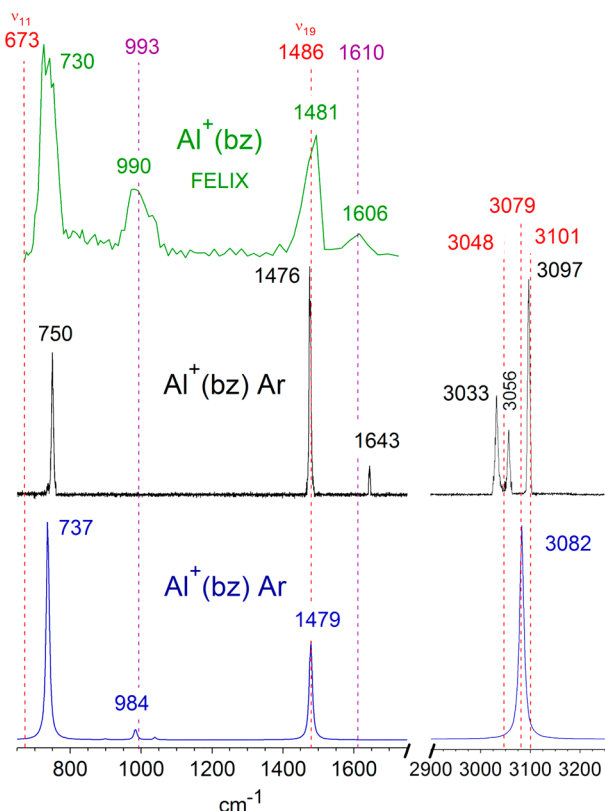


**Figure 3.** IR-REMPD spectrum of  $\text{Al}^+(\text{C}_6\text{H}_6)$  taken at FELIX compared to the photodissociation spectrum of  $\text{Al}^+(\text{C}_6\text{H}_6)\text{Ar}$  (this work) and the corresponding predicted spectrum. The red dashed lines represent the positions of free benzene IR bands, and the purple dashed lines indicate the positions of Raman active bands.

experiment and the B3LYP predictions. The differences between frequencies predicted by the two methods are perhaps understandable, because the two methods produce different metal-benzene bond distances and binding energies. Without some more sophisticated theoretical analysis beyond the scope of this paper, it is not completely clear why B3LYP produces better results.

Consistent with the previous FEL results, the spectrum for  $\text{Al}^+(\text{benzene})$  has two main bands in the fingerprint region. The vibration at  $1476\text{ cm}^{-1}$  is assigned to the  $\nu_{19}$  carbon ring distortion of benzene, whereas that at  $750\text{ cm}^{-1}$  is assigned to the  $\nu_{11}$  out-of-plane hydrogen bend.<sup>68,97</sup> Both of these strong features were also seen in the FEL spectrum at about the same positions, but the signal-to-noise levels and line widths are much improved in the present spectrum. The differences in band positions and widths presumably occur because the multiphoton dissociation process used for the FEL measurement induced line broadening and shifting. The FEL also had a line width of  $5\text{--}7\text{ cm}^{-1}$ , compared to that of  $1\text{--}2\text{ cm}^{-1}$  for the OPO laser used here. The relative intensities of the  $750$  and  $1476\text{ cm}^{-1}$  bands are different from those in the FEL spectrum and also different from those in the spectrum predicted by theory. This discrepancy can be explained partly by the pulse energy of the OPO, which declines significantly toward longer wavelengths. In principle, the spectrum could be corrected for this, but in practice this is very difficult because the OPO laser spot size and shape, and thus its overlap with the ion beam, varies as it scans. The spectra presented here are therefore not corrected for the OPO laser power. Another factor is that

theory predicts the absorption spectrum, whereas we measure the photodissociation spectrum; the photodissociation yield is also likely to decline toward lower energy, also depressing band intensities here. The FEL spectrum has a weaker band at  $990\text{ cm}^{-1}$ , assigned previously to the  $\nu_1$  vibration of benzene. It is predicted by theory to have much weaker intensity than the other bands, perhaps explaining why it is not detected here. Its greater intensity in the FEL spectrum may also be the result of some saturation in the multiphoton process. A much weaker band is detected in our spectrum at  $1643\text{ cm}^{-1}$  and assigned to the  $\nu_8$  vibration. This band is barely detected in the FEL spectrum and is not predicted by theory to have measurable intensity. It is not IR-active in benzene (and is therefore Raman active) but becomes very slightly active in metal complexes. In the region of the expected C–H stretch, which was not accessible with the FEL, our spectrum has a triplet of bands centered near the position predicted by theory. As noted earlier, benzene itself has a Fermi triad of bands here; the positions of these bands are indicated by the dashed red lines. This triad results from anharmonic interactions of overtones and combinations of lower frequency bands that are accidentally near-degenerate with the IR-active C–H stretch fundamental. Apparently, the binding of  $\text{Al}^+$  to benzene shifts these triad members slightly but does not change the frequencies enough to remove the degeneracy causing the Fermi resonance.

The shifts of the benzene vibrations that result from metal binding have been discussed previously and are reasonably well understood.<sup>46–52</sup> In the fingerprint region, the  $\nu_{11}$  out-of-plane bend usually shifts to higher frequency compared to this mode in benzene itself. This is attributed to a mechanical effect of increased repulsion at the outer turning point of the bend caused by the presence of the metal. Blue shifts of up to  $100\text{ cm}^{-1}$  were reported for this vibration in transition metal complexes studied previously.<sup>47,49</sup> In the present system, the band at  $750\text{ cm}^{-1}$  is  $77\text{ cm}^{-1}$  to the blue from the mode in benzene, a value quite comparable to those for other metal ion–benzene complexes.<sup>47,49</sup> This band is  $20\text{ cm}^{-1}$  to the blue from the band detected for  $\text{Al}^+(\text{benzene})$  in FEL experiments.<sup>48</sup> This is understandable because the multiphoton dissociation process often leads to red-shifting of vibrational bands.<sup>98</sup> The experimental blue shift is reproduced reasonably well by theory. The  $\nu_{19}$  mode in benzene usually shifts to lower frequencies in metal ion complexes because of ligand  $\rightarrow$  metal charge transfer.<sup>57</sup> This weakens the bonding in benzene and lowers the frequency of the ring distortion vibration. Red shifts of  $30\text{--}50\text{ cm}^{-1}$  were observed for transition metal ion–benzene complexes studied previously.<sup>47,49</sup> The previous FEL study of  $\text{Al}^+(\text{benzene})$  measured a broad band centered above the position of the free-molecule vibration, concluding that no shift could be measured within the uncertainty of the line width. Here, because the line width is much sharper, it is clear that the vibration in  $\text{Al}^+(\text{benzene})$  is slightly red-shifted by about  $10\text{ cm}^{-1}$  compared to this vibration in benzene. The small magnitude of this red shift, suggesting only a weak charge transfer interaction, is also reproduced reasonably well by theory. In addition to these vibrational band shifts, the other effect already mentioned is that bands having little or no IR intensity in benzene itself can gain intensity because of the reduction in symmetry and/or greater charge oscillation resulting from metal binding. This is the case here for the  $\nu_1$  band according to theory, but this band is not detected in our experiment. Theory does not predict measurable intensity for the  $\nu_8$  carbon ring stretch, but we apparently detect it at  $1643$

$\text{cm}^{-1}$ . This is a blue shift of  $33 \text{ cm}^{-1}$  from the corresponding band in benzene.

Figure 4 shows a comparison of the spectra for  $\text{Al}^+(\text{benzene})\text{Ar}$  and  $\text{Al}^+(\text{benzene})_2\text{Ar}$ , along with that predicted by theory

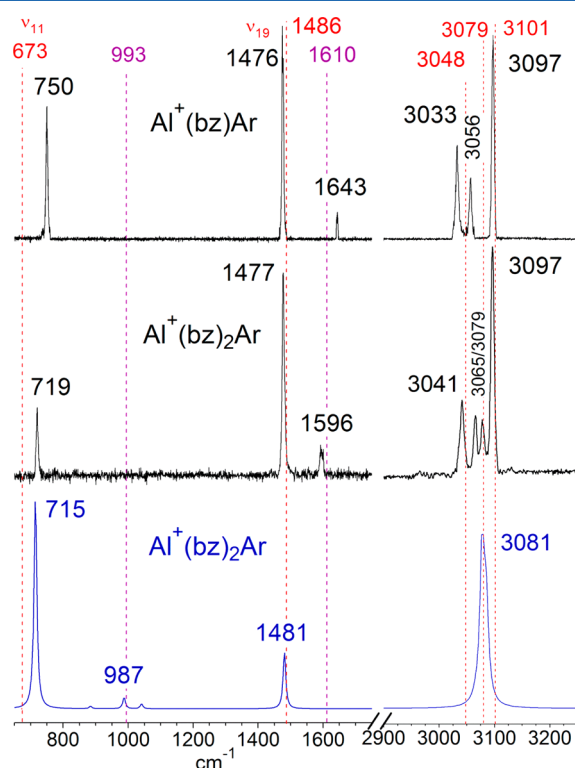


**Figure 4.** IR photodissociation spectra of  $\text{Al}^+(\text{C}_6\text{H}_6)_{1-2}\text{Ar}$  and the predicted spectrum of  $\text{Al}^+(\text{C}_6\text{H}_6)_2\text{Ar}$ . The red dashed lines represent the positions of free benzene IR bands, and the purple dashed lines indicate the positions of Raman active bands.

for the latter ion. The general features of these spectra are similar, but there are noticeable differences in the details. The  $\nu_{19}$  vibration appears at almost the same frequency for both complexes, consistent with the same kind of weak charge transfer interaction for both. The  $\nu_{11}$  vibration is blue-shifted for both complexes, but the shift is much smaller for the dibenzene system. This makes sense because the metal–benzene bond distances predicted by theory are longer for the dibenzene complex, which would reduce the repulsive interaction between the C–H bending motions and the metal. The  $\nu_8$  carbon ring stretch at  $1643 \text{ cm}^{-1}$  for  $\text{Al}^+(\text{benzene})\text{Ar}$  apparently has moved to lower frequency at  $1596 \text{ cm}^{-1}$  for the dibenzene complex. Again, this band has reasonable signal level in the experiment but is not predicted to have significant intensity by theory. Likewise, weak bands predicted near  $1000 \text{ cm}^{-1}$  are not detected. In the C–H stretching region, the monobenzene ion has a triplet of three bands, similar to the pattern for isolated benzene. The dibenzene complex, however, has four bands here. The highest frequency member of these two multiplets occurs at the same position for both complexes, but the lower frequency features are all slightly shifted. Apparently, the Fermi interactions here are somewhat different for these two ions, but the frequencies remain close enough so that the Fermi interaction still occurs. Consistent with this, the single C–H stretch predicted by harmonic theory occurs at virtually the same frequency for both complexes. The overall features of this spectrum indicate that

the dibenzene complex has noticeably different interactions than those for the monobenzene species. Although the patterns are consistent with those predicted by theory for a sandwich structure, there is really no distinctive signature of the bent-sandwich aspect of this structure that could be detected in the experiment.

The spectra of the mono- and dibenzene complexes are compared to that of the tribenzene complex in Figure 5. Again,

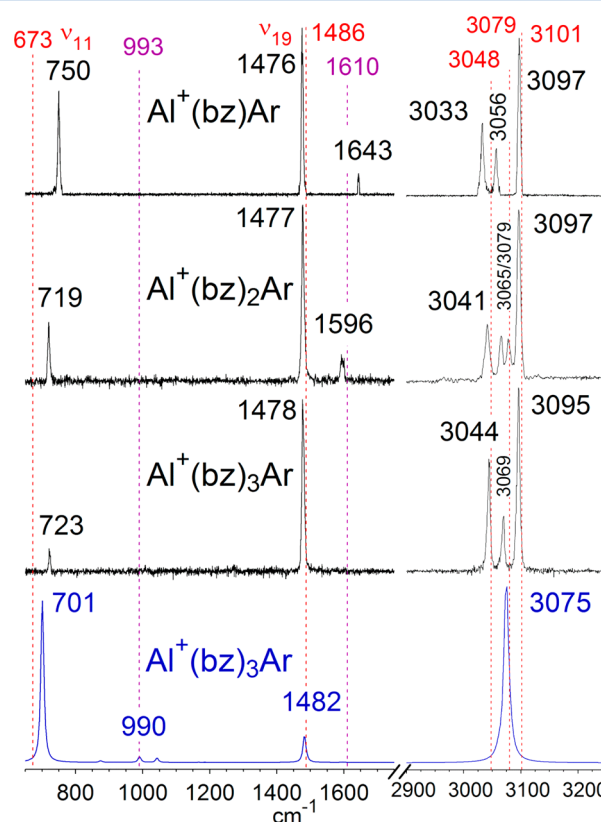


**Figure 5.** IR photodissociation spectra of  $\text{Al}^+(\text{C}_6\text{H}_6)_{1-3}\text{Ar}$  and the predicted spectrum of  $\text{Al}^+(\text{C}_6\text{H}_6)_3\text{Ar}$ . The red dashed lines represent the positions of free benzene IR bands, and the purple dashed lines indicate the positions of Raman active bands.

these spectra are more similar than they are different, but slight variations are apparent. The  $\nu_{19}$  vibration is again in almost the same position as that for isolated benzene, although there is a trend such that the red shift is greatest for the monobenzene complex and less for the di- and triligand species. This trend is also reproduced by theory. The  $\nu_{11}$  vibration had a greater blue shift for the monobenzene complex and a smaller one for the dibenzene system, but this vibration shifts back to the blue by several  $\text{cm}^{-1}$  for the tribenzene species. Another change is that the  $\nu_8$  vibration seen at  $1643$  and  $1596 \text{ cm}^{-1}$  for the mono- and dibenzene complexes is not seen at all for the tribenzene species. The C–H stretching region for the tribenzene complex has a triplet like that of the monobenzene system, but the shift for each of these features relative to the isolated benzene bands is quite small. The smaller shifts ( $\nu_{19}$  band and C–H triad) and reduced intensities ( $\nu_8$  band) suggest a weaker interaction between the cation and benzene in the triligand complex, consistent with the longer metal–ligand bond distances predicted by theory. The only band with a greater shift is that for the  $\nu_{11}$  vibration. This also makes sense for the three-coordinate structure predicted by theory, which has C–H

moieties on adjacent benzenes quite close to each other. Repulsive interactions here could also hinder the bending motions in the same way that the metal ion does, resulting in the small additional shift to higher frequency. Theory predicts a blue shift for this vibration but does not capture its magnitude very well.

The three-coordinate configuration predicted by theory for the tribenzene complex is somewhat surprising, and it would be nice to have definitive proof of this structure. Unfortunately, however, no striking change in the vibrational structure is predicted by theory for this arrangement of the ligands, and none is seen. However, if the structure was that of a dibenzene core with an external benzene not interacting with the metal, the spectrum would be more like that of the dibenzene complex. It does not seem likely that the  $\nu_8$  ring vibration would suddenly lose its IR intensity, nor that the quartet in the C–H region would get more simple by adding an external ligand. Our computations attempted to investigate a “2 + 1” structure, with one external benzene, but this structure did not converge. However, according to our theory for the  $n = 4$  complex, which does have one external ligand (see Supporting Information and discussion below), a dibenzene sandwich isomer with an external benzene should have an additional band for the  $\nu_{11}$  vibration from the external benzene. We do not see any doubling of this band, and therefore conclude that the spectral data and shift patterns are consistent with the three-coordinate structure.

Figure 6 shows the spectrum of the  $\text{Al}^+(\text{benzene})_4$  complex, measured in the mass channel corresponding to the elimination of benzene, compared to the predictions of theory for this complex and to the spectrum of  $\text{Al}^+(\text{benzene})_3\text{Ar}$ . These two spectra are virtually identical, except that the band at  $723\text{ cm}^{-1}$

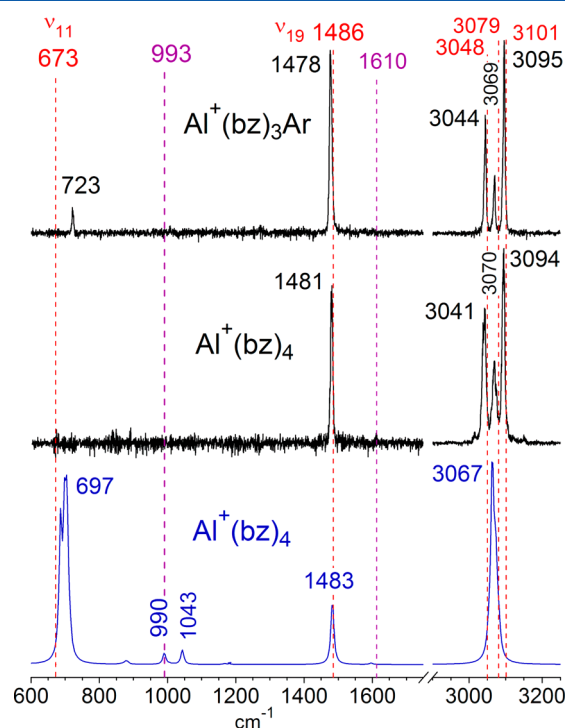


**Figure 6.** IR photodissociation spectra of  $\text{Al}^+(\text{C}_6\text{H}_6)_3\text{Ar}$  and  $\text{Al}^+(\text{C}_6\text{H}_6)_4$  and the predicted spectrum of  $\text{Al}^+(\text{C}_6\text{H}_6)_4$ . The red dashed lines represent the positions of free benzene IR bands, and the purple dashed lines indicate the positions of Raman active bands.

for  $\text{Al}^+(\text{benzene})_3\text{Ar}$  is not detected in the  $\text{Al}^+(\text{benzene})_4$  spectrum. This is most likely because of the lower photodissociation efficiency at this low energy. The  $n = 4$  complex tagged with argon could not be produced with great enough concentration to study, and therefore we could only measure this spectrum via the elimination of benzene. However, the benzene binding energy (computed to be  $10.9\text{ kcal/mol}$  by DFT/B97-D) is much greater than that of argon, and the photon energy may not be enough to eliminate this at the low energy. Interestingly,  $\text{Al}^+(\text{benzene})_4$  does photodissociate at the  $1481\text{ cm}^{-1}$  energy of the  $\nu_{19}$  band. If this photodissociation is a one-photon event (likely because of the low laser power), then this sets an experimental upper limit on the “solvent” benzene binding energy of this cluster at  $4.2\text{ kcal/mol}$ . Surprisingly, this is significantly less than the computed B97-D value and more in line with the B3LYP value ( $2.8\text{ kcal/mol}$ ). We have also used the elimination of such external ligands to measure IR spectra in the case of several metal cation–carbonyl complexes.<sup>89</sup>

If the structures predicted by theory are correct, then  $\text{Al}^+(\text{benzene})_4$  should have a core of three-coordinate  $\text{Al}^+(\text{benzene})_3$  with one external benzene acting as a solvent. The vibrational patterns of core versus external ligands have been discussed extensively in our studies of other metal ion–molecular complexes.<sup>50,89,90,93–96</sup> The nature of these vibrations in metal–benzene complexes have been discussed in our recent study of  $\text{Ni}^+(\text{benzene})_n$ .<sup>65</sup> In most systems, ligands attached to a metal ion have vibrations that are shifted with respect to those of the free molecule, whereas vibrations in the second sphere are more like those of the free molecule. In the present system, the distinction between the spectra for the two types of ligands is difficult to make because the shifts on inner-sphere ligand vibrations here are so small. In the spectra predicted by theory, the external benzene molecule does have distinct vibrations, but the frequencies of these overlap those of the core ligands for the  $\nu_{19}$  vibration and for the C–H stretch. Not surprisingly, we cannot detect any doubling of the bands in these regions. For the  $\nu_{11}$  vibration at much lower frequency, theory does predict a large difference between the core and external ligand frequencies, resulting in a predicted doublet at this position, but this is the region where we do not detect the bands. Unfortunately, therefore, the vibrational patterns for the  $n = 4$  complex are just not definitive in identifying the expected external benzene.

Additional spectral data for these aluminum–benzene clusters can be obtained in the higher frequency region above the C–H stretching vibrations. Solid benzene is known to exhibit combination bands in this region of the spectrum,<sup>99</sup> and such bands may also be found for these aluminum–benzene complexes. Figure 7 shows the spectra for the different sized complexes in this higher frequency region, with dashed red lines to indicate the bands at  $3645$ ,  $3695$ , and  $4050\text{ cm}^{-1}$  known for benzene in solid crystals.<sup>99</sup> Harmonic theory does not predict these combination bands, and so we can only attempt assignment with simple mathematical addition of fundamental bands, as has been done in the previous work.<sup>99</sup> In that previous work, the bands at  $3645$  and  $3695\text{ cm}^{-1}$  were assigned to a  $\nu_6$  (carbon ring deformation) combination with the two main bands in the C–H Fermi triad; the intervals match almost perfectly with the  $606\text{ cm}^{-1}$  frequency for this vibration. The  $4050\text{ cm}^{-1}$  band lies about  $1000\text{ cm}^{-1}$  above the Fermi triad and was not assigned in the previous work because there are several vibrational intervals that could produce a band here.  $\text{Al}^+(\text{benzene})\text{Ar}$  has no bands in this higher frequency



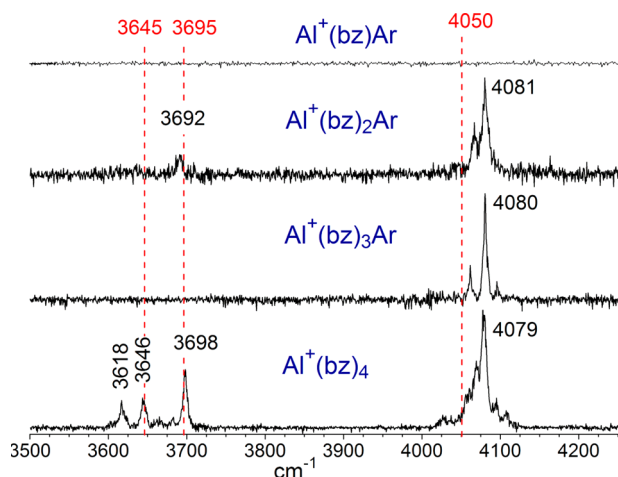


**Figure 7.** Combination bands seen in the higher frequency region in the IR photodissociation spectra of  $\text{Al}^+(\text{C}_6\text{H}_6)_{1-3}\text{Ar}$  and  $\text{Al}^+(\text{C}_6\text{H}_6)_4$ . The red dashed lines correspond to the positions of bands observed previously in the IR spectrum of liquid benzene.

region. Presumably, the perturbation on benzene modes induced by the stronger metal ion bonding shifts vibrations and/or reduces the couplings that generate these combination bands. However, all the larger complexes have one or more bands in this region, in approximately the positions seen for isolated benzene. The  $\text{Al}^+(\text{benzene})_2\text{Ar}$  and  $\text{Al}^+(\text{benzene})_3\text{Ar}$  complexes have little or no structure in the 3600–3700  $\text{cm}^{-1}$  region, but all three larger clusters have doublet-like bands near 4080  $\text{cm}^{-1}$ . This latter feature is somewhat higher in frequency than the band seen for crystalline benzene but does not change significantly with complex size. The most interesting aspect of these spectra is the sudden appearance of well-defined structure in the lower frequency region for  $\text{Al}^+(\text{benzene})_4$ , with bands at 3618, 3646, and 3698  $\text{cm}^{-1}$ . The latter two of these fall at almost exactly the positions of bands seen for isolated benzene. The sudden onset of signal here, and the band positions matching those for isolated benzene, are consistent with the presence of an external benzene molecule beginning at this cluster size. This is perhaps our best experimental evidence for the external benzene.

The picture of aluminum cation–benzene bonding that emerges from this study is one of relatively weak electrostatic interactions. The binding of benzene to metal is through cation– $\pi$  electrostatic interactions rather than the covalent bonding that dominates for transition metal–benzene complexes. These interactions have been discussed greatly in the context of biology,<sup>4–8</sup> but there are few direct spectroscopic probes of their influence on structure and spectra. In addition to the cation– $\pi$  interactions, other electrostatic forces (quadrupole–quadrupole, dispersion) undoubtedly play a role, particularly for the second-sphere molecule in the  $n = 4$  complex. This is illustrated by the significant bond energy differences between the B3LYP and B97-D calculations. Future work could use energy component analysis, as has been done for pure benzene clusters, to decompose the various contributions to the bonding and their magnitudes.<sup>100</sup> Unfortunately, except for the  $n = 4$  complex, no insight is gained from this study into the cation–benzene dissociation energies of these complexes. However, these studies rely throughout on the very weak cation bonding interactions with argon. Our calculations with DFT are probably not particularly

reliable on these values, but the  $\text{Al}^+(\text{benzene})_n\text{–Ar}$  dissociation energies are predicted to be less than 1 kcal/mol. Our experiment finds that argon is eliminated from these complexes when we excite the  $\nu_{11}$  vibration just above 700  $\text{cm}^{-1}$  (equivalent to 2 kcal/mol). The band position of each of these vibrations therefore places an upper limit on the argon binding energies for each complex. It is worth noting that similar studies employing argon tagging in the fingerprint region will be considerably more difficult for transition metal ions, which bind argon much more strongly. For future studies of these systems, tagging should employ more weakly bound spectator atoms such as neon.

The vibrational patterns of these complexes provide some insight into their electrostatic bonding. As noted in previous work, the key vibration determining the extent of charge transfer between benzene and attached cations is the  $\nu_{19}$  vibration. In transition metal ion complexes with stronger covalent bonding, this vibration may shift as much as 100  $\text{cm}^{-1}$  to the red from its isolated benzene value. However, this vibration is shifted by  $\leq 10 \text{ cm}^{-1}$  in the aluminum complexes described here. The  $\nu_{11}$  vibration in these aluminum complexes shifts to the blue by about the same amount as that seen for transition metal complexes, but this shift has a mechanical origin rather than one from bonding interactions and its magnitude is therefore understandable. The spectroscopic patterns measured are consistent with those predicted by theory, and this same theory suggests weak bonding energies.

The spectra measured here are completely consistent with the structures predicted by theory for these complexes. The dibenzene and tribenzene complexes have single bands at each of the vibrations in the fingerprint region. This is consistent with all ligands in these complexes having the same coordination, with each ligand bound directly to the metal. The 3-fold coordination in the  $n = 3$  complex is further supported by the fragmentation patterns. The trend in the shift of the  $\nu_{11}$  vibration also provides additional circumstantial evidence for this. The 3-fold coordination around  $\text{Al}^+$  is of course different from the coordination seen for familiar transition metal ion complexes. However, this same coordination has been seen previously in computational studies of alkali cation–benzene complexes, where the interaction is also electrostatic.<sup>60–62</sup> The bent sandwich structures predicted for the  $n = 2$  and 3 complexes here are consistent with similar bent structures seen in the past for other aluminum cation–molecule complexes.<sup>70,71,74</sup> Unfortunately, however, this aspect of these structures cannot be confirmed by this study, as there is no distinct signature for this in the vibrational patterns.

## CONCLUSIONS

The coordination versus solvation behavior in  $\text{Al}^+(\text{benzene})_n$  complexes ( $n = 1\text{--}4$ ) is studied here with infrared photodissociation spectroscopy of mass-selected ions in the region 600–4200  $\text{cm}^{-1}$ . Because of the cation–benzene bond energies, these experiments are only possible with the method of argon tagging. This is particularly critical for measurements in the low energy region of the fingerprint region and is only possible here because of the low binding energies between  $\text{Al}^+$  and argon. These spectroscopic studies are complemented by computational studies with density functional theory. The bonding in these complexes is much weaker than that found for transition metal ions, and the key vibration ( $\nu_{19}$ ) indicating charge transfer exhibits bands that are only slightly shifted from the frequency in isolated benzene. These complexes are



therefore concluded to be bound by relatively weak cation- $\pi$  electrostatic interactions, consistent with those found for other aluminum ion-molecule complexes. The vibrational patterns are not completely definitive for the coordination around the aluminum cation, but the combined data are consistent with the 3-fold coordination predicted by theory. The fourth benzene molecule acts as a solvent, bound primarily by CH- $\pi$  hydrogen bonds donated by two of the coordinated molecules. Infrared OPO measurements with rare gas tagging of the ions provide an improvement on multiphoton studies done in the past on metal-benzene complexes in the fingerprint region, but the binding energy of the rare gas atoms is a concern for future studies of transition metal complexes at the lowest energies.

## ■ ASSOCIATED CONTENT

### ■ Supporting Information

The full citation for refs 86 and 87. Mass spectra, IR spectra, and additional details on the DFT computations, including the structures, energetics, and vibrational frequencies for each of the structures considered. This material is available free of charge via the Internet at <http://pubs.acs.org>.

## ■ AUTHOR INFORMATION

### Corresponding Author

\*M. A. Duncan: e-mail, [maduncan@uga.edu](mailto:maduncan@uga.edu); fax, 706-542-1234.

### Notes

The authors declare no competing financial interest.

## ■ ACKNOWLEDGMENTS

We acknowledge generous support for this work from the U.S. Department of Energy, Office of Science, Basic Energy Sciences, Division of Chemical, Geological, and Biosciences (grant no. DE-FG02-96ER14658).

## ■ REFERENCES

- (1) Long, N. J. *Metalloenes*; Blackwell Sciences: Oxford, U.K., 1998.
- (2) Hartwig, J. In *Organotransition Metal Chemistry: From Bonding to Catalysis*; Murzdek, J., Ed.; University Science Books: Sausalito, CA, 2010.
- (3) Fritz, H. P. Infrared and Raman Spectral Studies of  $\pi$ -Complexes Formed between Metals and  $C_nH_n$  Rings. *Adv. Organomet. Chem.* **1964**, *1*, 239–316.
- (4) Ma, J. C.; Dougherty, D. A. The Cation- $\pi$  Interaction. *Chem. Rev.* **1997**, *97*, 1303–1324.
- (5) Kim, D.; Hu, S.; Tarakeshwar, P.; Kim, K. S.; Lisy, J. M. Cation- $\pi$  Interactions: A Theoretical Investigation of the Interaction of Metallic and Organic Cations with Alkenes, Arenes, and Heteroarenes. *J. Phys. Chem. A* **2003**, *107*, 1228–1238.
- (6) Dougherty, D. A. The Cation- $\pi$  Interaction. *Acc. Chem. Res.* **2013**, *46*, 885–893.
- (7) Watt, M. M.; Collins, M. S.; Johnson, D. W. Ion- $\pi$  Interactions in Ligand Design for Anions and Main Group Cations. *Acc. Chem. Res.* **2013**, *46*, 955–966.
- (8) Mahadevi, A. S.; Sastry, G. N. Cation- $\pi$  Interaction: Its Role and Relevance in Chemistry, Biology and Materials Science. *Chem. Rev.* **2013**, *113*, 2100–2138.
- (9) Russell, D. H., Ed. *Gas Phase Inorganic Chemistry*; Plenum Press: New York, 1989.
- (10) Eller, K.; Schwarz, H. Organometallic Chemistry in the Gas Phase. *Chem. Rev.* **1991**, *91*, 1121–1171.
- (11) Freiser, B. S., Ed. *Organometallic Ion Chemistry*; Kluwer Academic Publishers: Dordrecht, The Netherlands, 1996.
- (12) Duncan, M. A. Spectroscopy of Metal Ion Complexes: Gas Phase Models for Solvation. *Annu. Rev. Phys. Chem.* **1997**, *48*, 69–93.
- (13) Nakajima, A.; Kaya, K. A Novel Network Structure of Organometallic Clusters in the Gas Phase. *J. Phys. Chem. A* **2000**, *104*, 176–191.
- (14) Duncan, M. A. Frontiers in the Spectroscopy of Mass-Selected Molecular Ions. *Int. J. Mass Spectrom.* **2000**, *200*, 545–569.
- (15) Duncan, M. A., Ed. *Metal Ion Solvation and Metal-Ligand Interactions, Adv. Metal Semicon. Clusters*; Elsevier: Amsterdam, 2001; Vol. 5.
- (16) Leary, J. J.; Armentrout, P. B., Eds. *Gas Phase Metal Ion Chemistry* (special issue). *Int. J. Mass Spectrom.* **2001**, *204*, 1–294.
- (17) MacAleese, L.; Maitre, P. Infrared Spectroscopy of Organometallic Ions in the Gas Phase: From Model to Real World Complexes. *Mass Spectrom. Rev.* **2007**, *26*, 583–605.
- (18) Duncan, M. A. Structures, Energetics and Spectroscopy of Gas Phase Transition Metal Ion-Benzene Complexes. *Int. J. Mass Spectrom.* **2008**, *272*, 99–118.
- (19) Hoshino, K.; Kurikawa, T.; Takeda, H.; Nakajima, A.; Kaya, K. Structures and Ionization Energies of Sandwich Clusters ( $V_n(\text{Benzene})_m$ ). *J. Phys. Chem.* **1995**, *99*, 3053–3055.
- (20) Kurikawa, T.; Hirano, M.; Takeda, H.; Yagi, K.; Hoshino, K.; Nakajima, A.; Kaya, K. Structures and Ionization Energies of Cobalt-Benzene Clusters ( $Co_n(\text{Benzene})_m$ ). *J. Phys. Chem.* **1995**, *99*, 16248–16252.
- (21) Kurikawa, T.; Takeda, H.; Hirano, M.; Judai, K.; Arita, T.; Nagao, S.; Nakajima, A.; Kaya, K. Electronic Properties of Organometallic Metal-Benzene Complexes [ $M_n(\text{Benzene})_m$  ( $M = \text{Sc}–\text{Cu}$ )]. *Organometallics* **1999**, *18*, 1430–1438.
- (22) Weis, P.; Kemper, P. R.; Bowers, M. T. Structures and Energetics of  $V_n(C_6H_6)_m^+$  Clusters: Evidence for a Quintuple-Decker Sandwich. *J. Phys. Chem. A* **1997**, *101*, 8207–8213.
- (23) Chen, Y. M.; Armentrout, P. B. Collision-Induced Dissociation of Silver Benzene Cation  $Ag(C_6H_6)^+$ . *Chem. Phys. Lett.* **1993**, *210*, 123–128.
- (24) Meyer, F.; Khan, F. A.; Armentrout, P. B. Thermochemistry of Transition Metal Benzene Complexes: Binding Energies of  $M-(C_6H_6)_x^+$  ( $x = 1, 2$ ) for  $M = \text{Ti}$  to  $\text{Cu}$ . *J. Am. Chem. Soc.* **1995**, *117*, 9740–9748.
- (25) Rogers, M. T.; Armentrout, P. B. Noncovalent Metal-Ligand Bond Energies as Studied by Threshold Collision-Induced Dissociation. *Mass Spectrom. Rev.* **2000**, *19*, 215–247.
- (26) Amicangelo, J. C.; Armentrout, P. B. Absolute Binding Energies of Alkali-Metal Cation Complexes with Benzene Determined by Threshold Collision-Induced Dissociation Experiments and Ab Initio Theory. *J. Phys. Chem. A* **2000**, *104*, 11420–11432.
- (27) Li, Y.; Baer, T. Dissociation Kinetics of Energy-Selected  $(C_6H_6)_2Cr^+$  Ions: Benzene-Chromium Neutral and Ionic Bond Energies. *J. Phys. Chem. A* **2002**, *106*, 9820–9826.
- (28) Dunbar, R. C.; Klippenstein, S. J.; Hrusak, J.; Stockigt, D.; Schwarz, H. Binding Energy of  $Al(C_6H_6)^+$  from Analysis of Radiative Association Kinetics. *J. Am. Chem. Soc.* **1996**, *118*, 5277–5283.
- (29) Hettich, R. L.; Jackson, T. C.; Stanko, E. M.; Freiser, B. S. Gas-Phase Photodissociation of Organometallic Ions: Bond Energy and Structure Determinations. *J. Am. Chem. Soc.* **1986**, *108*, 5086–5093.
- (30) Gord, J. R.; Freiser, B. S.; Buckner, S. W. Kinetic Energy Release in Thermal Ion-Molecule Reactions: The  $Nb_2^+(\text{benzene})$  Single Charge-Transfer Reaction. *J. Chem. Phys.* **1991**, *94*, 4282–4290.
- (31) Afzaal, S.; Freiser, B. S. Gas-Phase Photodissociation Study of  $Ag(\text{benzene})^+$  and  $Ag(\text{toluene})^+$ . *Chem. Phys. Lett.* **1994**, *218*, 254–260.
- (32) Willey, K. F.; Cheng, P. Y.; Pearce, K. D.; Duncan, M. A. Photoinitiated Charge Transfer and Dissociation in Mass-Selected Metallo-Organic Complexes. *J. Phys. Chem.* **1990**, *94*, 4769–4772.
- (33) Willey, K. F.; Cheng, P. Y.; Bishop, M. B.; Duncan, M. A. Charge Transfer Photochemistry in Ion-Molecule Cluster Complexes of Silver. *J. Am. Chem. Soc.* **1991**, *113*, 4721–4728.
- (34) Willey, K. F.; Yeh, C. S.; Robbins, D. L.; Duncan, M. A. Charge Transfer in the Photodissociation of Metal Ion-Benzene Complexes. *J. Phys. Chem.* **1992**, *96*, 9106–9111.

- (35) Buchanan, J. W.; Grieves, G. A.; Reddic, J. E.; Duncan, M. A. Novel Mixed Ligand Sandwich Complexes: Competitive Binding of Iron with Benzene, Coronene, and  $C_{60}$ . *Int. J. Mass Spectrom.* **1999**, *182*, 323–333.
- (36) Jaeger, T. D.; Duncan, M. A. Photodissociation of  $M^+(\text{Benzene})_x$  Complexes ( $M = \text{Ti, V, Ni}$ ) at 355 nm. *Int. J. Mass Spectrom.* **2005**, *241*, 165–171.
- (37) Pillai, E. D.; Molek, K. S.; Duncan, M. A. Growth and Photodissociation of  $U^+(\text{C}_6\text{H}_6)_n$  ( $n = 1-3$ ) and  $\text{UO}_m^+(\text{C}_6\text{H}_6)$  ( $m = 1, 2$ ) Complexes. *Chem. Phys. Lett.* **2005**, *405*, 247–251.
- (38) Walker, N. R.; Wright, R. R.; Stace, A. J. Stable  $\text{Ag}(\text{II})$  Coordination Complexes in the Gas Phase. *J. Am. Chem. Soc.* **1999**, *121*, 4837–4844.
- (39) Ma, L.; Takashima, T.; Koka, J.; Kimber, H. J.; Cox, H.; Stace, A. J. Conformation-Resolved UV Spectra of  $\text{Pb}(\text{II})$  Complexes: A Gas Phase Study of the Sandwich Structures  $[\text{Pb}(\text{Toluene})_2]^{2+}$  and  $[\text{Pb}(\text{Benzene})_2]^{2+}$ . *J. Chem. Phys.* **2013**, *138*, 164301/1–11.
- (40) Sohnlein, B. R.; Li, S. G.; Yang, D.-S. Electron-Spin Multiplicities and Molecular Structures of Neutral and Ionic Scandium-Benzene Complexes. *J. Chem. Phys.* **2005**, *123*, 214306/1–7.
- (41) Sohnlein, B. R.; Lei, Y. X.; Yang, D.-S. Electronic States of Neutral and Cationic Bis(Benzene) Titanium and Vanadium Sandwich Complexes Studied by Pulsed Field Ionization Electron Spectroscopy. *J. Chem. Phys.* **2007**, *127*, 114302/1–10.
- (42) Yang, D. S. High-Resolution Electron Spectroscopy of Gas-Phase Metal-Aromatic Complexes. *J. Phys. Chem. Lett.* **2011**, *2*, 25–33.
- (43) Lei, Y.; Wu, L.; Sohnlein, B. R.; Yang, D.-S. High-Spin Electronic States of Lanthanide-Arene Complexes:  $\text{Nd}(\text{Benzene})$  and  $\text{Nd}(\text{Naphthalene})$ . *J. Chem. Phys.* **2012**, *136*, 204311/1–7.
- (44) Liu, Y.; Kumari, S.; Roudjane, M.; Li, S. G.; Yang, D.-S. Electronic States and Pseudo Jahn-Teller Distortion of Heavy Metal-Monobenzene Complexes:  $M(\text{C}_6\text{H}_6)$  ( $M = \text{Y, La, and Lu}$ ). *J. Chem. Phys.* **2012**, *136*, 134310/1–9.
- (45) Han, S.; Singh, N. J.; Kang, T. Y.; Choi, K.-W.; Choi, S.; Baek, S. J.; Kim, K. S.; Kim, S. K. Aromatic  $\pi$ - $\pi$  Interaction Mediated by a Metal Atom: Structure and Ionization of the Bis( $\eta^6$ -Benzene) Chromium-Benzene Cluster. *Phys. Chem. Chem. Phys.* **2010**, *12*, 7648–7653.
- (46) Cabarcos, O. M.; Weinheimer, C. J.; Lisy, J. M. Size Selectivity by Cation- $\pi$  Interactions: Solvation of  $\text{K}^+$  and  $\text{Na}^+$  by Benzene and Water. *J. Chem. Phys.* **1999**, *110*, 8429–8435.
- (47) van Heijnsbergen, D.; von Helden, G.; Meijer, G.; Maitre, P.; Duncan, M. A. Infrared Spectra of Gas-Phase  $\text{V}^+(\text{Benzene})$  and  $\text{V}^+(\text{Benzene})_2$  Complexes. *J. Am. Chem. Soc.* **2002**, *124*, 1562–1563.
- (48) van Heijnsbergen, D.; Jaeger, T. D.; von Helden, G.; Meijer, G.; Duncan, M. A. The Infrared Spectrum of  $\text{Al}^+$ -Benzene in the Gas Phase. *Chem. Phys. Lett.* **2002**, *364*, 345–351.
- (49) Jaeger, T. D.; van Heijnsbergen, D.; Klippenstein, S. J.; von Helden, G.; Meijer, G.; Duncan, M. A. Vibrational Spectroscopy and Density Functional Theory of Transition Metal Ion-Benzene and Dibenzene Complexes in the Gas Phase. *J. Am. Chem. Soc.* **2004**, *126*, 10981–10991.
- (50) Duncan, M. A. Infrared Spectroscopy to Probe Structure and Dynamics in Metal Ion-Molecule Complexes. *Int. Rev. Phys. Chem.* **2003**, *22*, 407–435.
- (51) Jaeger, T. D.; Pillai, E. D.; Duncan, M. A. Structure, Coordination and Solvation of  $\text{V}^+(\text{Benzene})_n$  Complexes via Gas Phase Infrared Spectroscopy. *J. Phys. Chem. A* **2004**, *108*, 6605–6610.
- (52) Jaeger, T. D.; Duncan, M. A. Vibrational Spectroscopy of  $\text{Ni}^+(\text{Benzene})_n$  Complexes in the Gas Phase. *J. Phys. Chem. A* **2005**, *109*, 3311–3317.
- (53) Bauschlicher, C. W.; Partridge, H.; Langhoff, S. R. Theoretical Study of Transition-Metal Ions Bound to Benzene. *J. Phys. Chem.* **1992**, *96*, 3273–3278.
- (54) Stockigt, D. Cation- $\pi$  Interaction in  $\text{Al}(\text{L})^+$  Complexes ( $\text{L} = \text{C}_6\text{H}_6, \text{C}_3\text{H}_5\text{N}, \text{C}_3\text{H}_6, \text{C}_4\text{H}_4\text{NH}, \text{C}_4\text{H}_4\text{O}$ ). *J. Phys. Chem. A* **1997**, *101*, 3800–3807.
- (55) Dargel, T. K.; Hertwig, R. H.; Koch, W. How Do Coinage Metal Ions Bind to Benzene? *Mol. Phys.* **1999**, *96*, 583–591.
- (56) Yang, C. N.; Klippenstein, S. J. Theory and Modeling of the Binding in Cationic Transition-Metal-Benzene Complexes. *J. Phys. Chem. A* **1999**, *103*, 1094–1103.
- (57) Chaquin, P.; Costa, D.; Lepetit, C.; Che, M. Structure and Bonding in a Series of Neutral and Cationic Transition Metal-Benzene  $\eta^6$  Complexes  $M(\eta^6\text{-C}_6\text{H}_6)^{n+}$  ( $M = \text{Ti, V, Cr, Fe, Co, Ni, and Cu}$ ). Correlation of Charge Transfer with the Bathochromic Shift of the  $e_1$  Ring Vibration. *J. Phys. Chem. A* **2001**, *105*, 4541–4545.
- (58) Pandey, R.; Rao, B. K.; Jena, P.; Blanco, M. A. Electronic Structure and Properties of Transition Metal-Benzene Complexes. *J. Am. Chem. Soc.* **2001**, *123*, 3799–3808.
- (59) Albertí, M.; Aguilar, A.; Lucas, J. M.; Pirani, F.; Cappelletti, D.; Coletti, C.; Re, N. Atom-Bond Pairwise Additive Representation for Cation-Benzene Potential Energy Surfaces: An Ab Initio Validation Study. *J. Phys. Chem. A* **2006**, *110*, 9002–9010.
- (60) Albertí, M.; Aguilar, A.; Pirani, F. Propensities in the Solvation of  $M^+$ -Benzene Systems ( $M = \text{Na, K, Rb}$ ) Investigated by Cluster Dynamics. *Chem. Phys.* **2012**, *399*, 290–295.
- (61) Marques, J. M. C.; Llanio-Trujillo, J. L.; Albertí, M.; Aguilar, A.; Pirani, F. Alkali-Ion Microsolvation with Benzene Molecules. *J. Phys. Chem. A* **2012**, *116*, 4947–4956.
- (62) Marques, J. M. C.; Llanio-Trujillo, J. L.; Albertí, M.; Aguilar, A.; Pirani, F. Microsolvation of the Potassium Ion with Aromatic Rings: Comparison Between Hexafluorobenzene and Benzene. *J. Phys. Chem. A* **2012**, *117*, 8043–8053.
- (63) Polestshuk, P. M.; Dem'yanov, P. I.; Ryabinkin, I. G. The Electronic Structure and Energetics of  $\text{V}^+$ -Benzene Half Sandwiches of Different Multiplicities: Comparative Multi-reference and Single-Reference Theoretical Study. *J. Chem. Phys.* **2008**, *129*, 054307/1–13.
- (64) Valencia, I.; Castro, M. Theoretical Study of the Structural and Electronic Properties of the  $\text{Fe}_n(\text{C}_6\text{H}_6)_m$ ,  $n \leq 2$ ;  $m \leq 2$  Complexes. *Phys. Chem. Chem. Phys.* **2010**, *12*, 7545–7554.
- (65) Castro, M.; Flores, R.; Duncan, M. A. Theoretical Study of Nascent Solvation in  $\text{Ni}^+(\text{Benzene})_m$ ,  $m = 3$  and 4, Clusters. *J. Phys. Chem. A* **2013**, *117*, 12546–12559.
- (66) Horváthová, L.; Dubecký, M.; Mitas, L.; Štich, I. Spin Multiplicity and Symmetry Breaking in Vanadium-Benzene Complexes. *Phys. Rev. Lett.* **2012**, *109*, 053001/1–5.
- (67) Horváthová, L.; Dubecký, M.; Mitas, L.; Štich, I. Quantum Monte Carlo Study of  $\pi$ -Bonded Transition Metal Organometallics: Neutral and Cationic Vanadium-Benzene and Cobalt-Benzene Half Sandwiches. *J. Chem. Theory Comput.* **2013**, *9*, 390–400.
- (68) Shimanouchi, T. Molecular Vibrational Frequencies, in *NIST Chemistry Webbook*; Linstrom, P. J.; Mallard, W. G., Eds.; NIST Standard Reference Database Number 69; National Institute of Standards and Technology: Gaithersburg MD, 20899 (<http://Webbook.Nist.Gov>).
- (69) Sodupe, M.; Bauschlicher, C. W.  $\text{Al}^+$ -Ligand Binding Energies. *Chem. Phys. Lett.* **1991**, *181*, 321–326.
- (70) Bauschlicher, C. W.; Partridge, H. The Bonding of Multiple Ligands to  $\text{Mg}^+$  and  $\text{Al}^+$ . *J. Phys. Chem.* **1991**, *95*, 9694–9698.
- (71) Kemper, P. R.; Bushnell, J.; Bowers, M. T.; Gellene, G. I. Binding between Ground-State Aluminum Ions and Small Molecules:  $\text{Al}^+(\text{H}_2/\text{CH}_4/\text{C}_2\text{H}_2/\text{C}_2\text{H}_4/\text{C}_2\text{H}_6)_n$ . Can  $\text{Al}^+$  Insert into  $\text{H}_2$ ? *J. Phys. Chem. A* **1998**, *102*, 8590–8597.
- (72) Chen, J.; Wong, T. H.; Kleiber, P. D.; Yang, K. H. Photofragmentation Spectroscopy of  $\text{Al}^+(\text{C}_2\text{H}_4)$ . *J. Chem. Phys.* **1999**, *110*, 11798–11805.
- (73) Agreiter, J. K.; Knight, A. M.; Duncan, M. A. ZEKE-PFI Spectroscopy of the  $\text{Al}(\text{H}_2\text{O})$  and  $\text{Al}(\text{D}_2\text{O})$  Complexes. *Chem. Phys. Lett.* **1999**, *313*, 162–170.
- (74) Inokuchi, Y.; Ohshimo, K.; Misaizu, F.; Nishi, N. Structures of  $[\text{Mg}(\text{H}_2\text{O})_{1,2}]^+$  and  $[\text{Al}(\text{H}_2\text{O})_{1,2}]^+$  Ions Studied by Infrared Photodissociation Spectroscopy: Evidence of  $[\text{HO-Al-H}]^+$  Ion Core Structure in  $[\text{Al}(\text{H}_2\text{O})_2]^+$ . *Chem. Phys. Lett.* **2004**, *390*, 140–144.
- (75) Lei, J.; Dagdigian, P. J. Electronic Spectroscopy of the  $\text{Al}^+$ -Ar Complex. *Chem. Phys. Lett.* **1999**, *304*, 317–322.

- (76) Duncan, M. A. Laser Vaporization Cluster Sources. *Rev. Sci. Instrum.* **2012**, *83*, 041101/1–19.
- (77) Duncan, M. A. Reflectron Time-of-Flight Mass Spectrometer for Laser Photodissociation. *Rev. Sci. Instrum.* **1992**, *63*, 2177–2186.
- (78) Bosenberg, W. R.; Guyer, D. R. Broadly Tunable, Single-Frequency Optical Parametric Frequency-Conversion System. *J. Opt. Soc. Am. B* **1993**, *10*, 1716–1722.
- (79) Gerhards, M.; Unterberg, C.; Gerlach, A. Structure of a  $\beta$ -Sheet Model System in the Gas Phase: Analysis of the C=O Stretching Vibrations. *Phys. Chem. Chem. Phys.* **2002**, *4*, 5563–5565.
- (80) Okumura, M.; Yeh, L. I.; Myers, J. D.; Lee, Y. T. Infrared Spectra of the Cluster Ions  $\text{H}_7\text{O}_3^+-\text{H}_2$  and  $\text{H}_9\text{O}_4^+-\text{H}_2$ . *J. Chem. Phys.* **1986**, *85*, 2328–2329.
- (81) Okumura, M.; Yeh, L. I.; Myers, J. D.; Lee, Y. T. Infrared Spectra of the Solvated Hydronium Ion: Vibrational Predissociation Spectroscopy of Mass-Selected  $\text{H}_3\text{O}^+(\text{H}_2\text{O})_n(\text{H}_2)_m$ . *J. Phys. Chem.* **1990**, *94*, 3416–3427.
- (82) Ebata, T.; Fujii, A.; Mikami, N. Vibrational Spectroscopy of Small-Sized Hydrogen-Bonded Clusters and their Ions. *Int. Rev. Phys. Chem.* **1998**, *17*, 331–361.
- (83) Bieske, E. J.; Dopfer, O. High-Resolution Spectroscopy of Cluster Ions. *Chem. Rev.* **2000**, *100*, 3963–3998.
- (84) Robertson, W. H.; Johnson, M. A. Molecular Aspects of Halide Hydration: The Cluster Approach. *Annu. Rev. Phys. Chem.* **2003**, *54*, 173–213.
- (85) Baer, T.; Dunbar, R. C. Ion Spectroscopy: Where Did It Come From, Where Is It Now, and Where Is It Going? *J. Am. Soc. Mass. Spectrom.* **2010**, *21*, 681–693.
- (86) Frisch, M. J.; et al. *Gaussian 03* (Revision B.02); Gaussian, Inc.: Pittsburgh, PA, 2003.
- (87) Schmidt, M. W.; et al. General Atomic and Molecular Electronic Structure System. *J. Comput. Chem.* **1993**, *14*, 1347–1363.
- (88) Gordon, M. S.; Schmidt, M. W. *Theory and Applications of Computational Chemistry*; Clifford, E. D., Gernot, F., Kwang, K. S., Scuseria, G. E., Eds.; Elsevier: Amsterdam, 2005; pp 1167–1189.
- (89) Ricks, A. M.; Duncan, M. A. Infrared Spectroscopy of Metal Carbonyl Cations. *J. Mol. Spectrosc.* **2011**, *266*, 63–74.
- (90) Bandyopadhyay, B.; Reishus, K. N.; Duncan, M. A. Infrared Spectroscopy of Solvation in Small  $\text{Zn}^+(\text{H}_2\text{O})_n$  Complexes. *J. Phys. Chem. A* **2013**, *117*, 7794–7803.
- (91) Hobza, P.; Müller-Dethlefs, K. *Non-Covalent Interactions*; RSC Publishing: Cambridge, U.K., 2010.
- (92) Cheng, T. C.; Bandyopadhyay, B.; Wheeler, S. E.; Duncan, M. A. Vibrational Spectroscopy and Theory of the Protonated Benzene Dimer and Trimer. *J. Phys. Chem. A* **2012**, *116*, 2065–7073.
- (93) Gregoire, G.; Brinkman, N. R.; Schaefer, H. F.; Duncan, M. A. Infrared Photodissociation Spectroscopy of  $\text{Mg}^+(\text{CO}_2)_n$  and  $\text{Mg}^+(\text{CO}_2)_n\text{Ar}_m$  Complexes. *J. Phys. Chem. A* **2003**, *107*, 218–227.
- (94) Walters, R. S.; Jaeger, T. D.; Brinkman, N. R.; Schaefer, H. F.; Duncan, M. A. Infrared Photodissociation Spectroscopy of  $\text{Al}^+(\text{CO}_2)_n$  and  $\text{Al}^+(\text{CO}_2)_n\text{Ar}_m$  Complexes. *J. Phys. Chem. A* **2003**, *107*, 7396–7405.
- (95) Jaeger, J. B.; Jaeger, T. D.; Brinkman, N. R.; Schaefer, H. F.; Duncan, M. A. Infrared Photodissociation Spectroscopy of  $\text{Si}^+(\text{CO}_2)_n$  and  $\text{Si}^+(\text{CO}_2)_n\text{Ar}$  Complexes. *Can. J. Chem.* **2004**, *82*, 934–946.
- (96) Brathwaite, A. D.; Duncan, M. A. Infrared Spectroscopy of  $\text{Si}(\text{CO})_n^+$  Complexes: Evidence for Asymmetric Coordination. *J. Phys. Chem. A* **2012**, *116*, 1375–1382.
- (97) We number the vibrations here for  $\text{Al}^+(\text{benzene})$  complexes according to the mode numbering for the isolated benzene molecule. Two different mode numbering schemes are common in the literature for the benzene molecule - the historical system first reported by Wilson, E. B. *Phys. Rev.* **1934**, *45*, 706–714 and the more recent “standard” system. We use the Wilson system.
- (98) von Helden, G.; van Heijnsbergen, D.; Meijer, G. Resonant Ionization using IR Light: A New Tool To Study the Spectroscopy and Dynamics of Gas-Phase Molecules. *J. Phys. Chem. A* **2003**, *107*, 1671–1688.
- (99) Mair, R. D.; Hornig, D. F. The Vibrational Spectra of Molecules and Complex Ions in Crystals. II. Benzene. *J. Chem. Phys.* **1949**, *17*, 1236–1247.
- (100) Sherrill, C. D. Energy Component Analysis of  $\pi$  Interactions. *Acc. Chem. Res.* **2013**, *46*, 1020–1028.